

Non-uniqueness, Counterrotation, and Negative Horizon Mass of Einstein-Maxwell-Chern-Simons Black Holes

Jutta Kunz and Francisco Navarro-Lérida

*Institut für Physik, Universität Oldenburg, Postfach 2503
D-26111 Oldenburg, Germany*

Stationary black holes in 5-dimensional Einstein-Maxwell-Chern-Simons theory possess surprising properties. When considering the Chern-Simons coefficient λ as a parameter, two critical values of λ appear: the supergravity value $\lambda_{\text{SG}} = 1$, and the value $\lambda = 2$. At $\lambda = 1$, supersymmetric black holes with vanishing horizon angular velocity, but finite angular momentum exist. As λ increases beyond λ_{SG} a rotational instability arises, and counterrotating black holes appear, whose horizon rotates in the opposite sense to the angular momentum. Thus supersymmetry is associated with the borderline between stability and instability. At $\lambda = 2$ rotating black holes with vanishing angular momentum emerge. Beyond $\lambda = 2$ black holes may possess a negative horizon mass, while their total mass is positive. Charged rotating black holes with vanishing gyromagnetic ratio appear, and black holes are no longer uniquely characterized by their global charges.

PACS Nos.: 04.20.Jb, 04.40.Nr

1. Introduction

Black holes in higher dimensions received much interest in recent years, in particular in the context of string theory, and with the advent of brane-world theories, raising the possibility of direct observation in future high energy colliders^{1,2}.

While the generalization of the Kerr metric to higher dimensions was obtained long ago³, the higher dimensional generalization of the Kerr-Newman solutions of Einstein-Maxwell (EM) theory is still not known analytically^{4,5}.

EM black holes in D dimensions are characterized by their mass M , charge Q , and $[(D-1)/2]$ angular momenta \mathbf{J} , their number corresponding to the rank of the rotation group $\text{SO}(D-1)$ ³. Their event horizon has surface gravity κ and $(D-2)$ -volume A_{H} , electrostatic potential Φ_{H} and $[(D-1)/2]$ angular velocities $\boldsymbol{\Omega}_{\text{H}}$. These black holes satisfy the Smarr formula⁶

$$M = \frac{(D-2)}{(D-3)8\pi G_D} \kappa A_{\text{H}} + \Phi_{\text{H}} Q + \frac{(D-2)}{(D-3)} \boldsymbol{\Omega}_{\text{H}} \cdot \mathbf{J}, \quad (1)$$

where G_D is the D -dimensional Newton constant, and the first law of black hole mechanics⁶,

$$dM = \frac{\kappa}{8\pi G_D} dA_{\text{H}} + \Phi_{\text{H}} dQ + \boldsymbol{\Omega}_{\text{H}} \cdot d\mathbf{J}. \quad (2)$$

In odd dimensions, $D = 2n + 1$, the EM action may be supplemented by a ‘ AF^n ’ Chern-Simons (CS) term. While not affecting the static black hole solutions, this term significantly affects the properties of stationary black hole solutions ^{7,8,6,9,10,11,12}, as discussed in this review.

The CS term also yields a modified Smarr formula, where Eq. (1) is supplemented by a further term, proportional to the CS coefficient λ and to the factor $(D - 5)$ ⁶. Thus $D = 5$ is a rather special case among the class of odd-dimensional Einstein-Maxwell-Chern-Simons (EMCS) theories, since the Smarr formula Eq. (1) remains unmodified.

The bosonic sector of minimal $D = 5$ supergravity may be viewed as a special case of the general EMCS theory with Lagrangian

$$\mathcal{L} = \frac{1}{16\pi G_5} \sqrt{-g} \left[R - F^2 + \frac{2\lambda}{3\sqrt{3}} \epsilon^{\mu\nu\rho\sigma\tau} A_\mu F_{\nu\rho} F_{\sigma\tau} \right], \quad (3)$$

and CS coefficient λ , where λ assumes the supergravity value $\lambda_{\text{SG}} = 1$. When $\lambda = 1$, analytic solutions describing charged, rotating black holes are known ^{7,8,13,14,15}. In contrast, for $\lambda \neq 1$ charged rotating black hole solutions are known only numerically ^{11,12}.

The extremal limits of rotating charged black hole solutions of $D = 5$ EMCS theory with $\lambda = 1$ are of special interest, since they encompass a two parameter family of stationary supersymmetric black holes ^{7,8}. The mass of these supersymmetric black holes is determined in terms of their charge and saturates the bound ¹⁶

$$M \geq \frac{\sqrt{3}}{2} |Q|, \quad (4)$$

while their two equal-magnitude angular momenta, $|J| = |J_1| = |J_2|$, are finite and satisfy the bound ^{8,10}

$$|J|^2 \leq \frac{1}{6\sqrt{3}\pi} |Q|^3, \quad (5)$$

in units for which $G_5 = 1$. Their horizon angular velocities Ω_{H} , however, vanish. Thus their horizon is non-rotating, although their angular momentum is nonzero. Clearly, angular momentum is stored in the Maxwell field, but surprisingly, a negative fraction of the total angular momentum is stored behind the horizon ^{6,10}. The effect of rotation on the horizon is not to make it rotate but to deform it into a squashed 3-sphere ⁶.

These special properties of $D = 5$ supersymmetric EMCS black holes caused speculations on how the properties of $D = 5$ black holes in general EMCS theories depend on the CS coefficient ⁶, involving instability and counterrotation of black holes beyond $\lambda = 1$. Both these features turned out to be true ¹¹. Moreover further intriguing features appeared at and beyond the second critical value $\lambda = 2$, involving non-uniqueness of black holes, the appearance of non-static black holes with vanishing total angular momentum, as well as the presence of black holes with negative horizon mass.

2. Properties of 5D EMCS Black Holes

To obtain stationary EMCS black hole solutions, we consider black hole space-times with bi-azimuthal symmetry, implying the existence of three commuting Killing vectors, $\xi = \partial_t$, $\eta_1 = \partial_{\varphi_1}$, and $\eta_2 = \partial_{\varphi_2}$ ^{3,17}.

While generic EMCS black holes possess two independent angular momenta, we here restrict to black holes whose angular momenta have equal magnitude. The metric and the gauge field parametrization then simplify. In particular, for such equal-magnitude angular momenta black holes, the general Einstein and gauge field equations reduce to a set of ordinary differential equations ⁴, since the angular dependence can be treated explicitly.

2.1. Metric and gauge potential

We employ a parametrization for the metric based on bi-azimuthal isotropic coordinates, well suited for the numerical construction ^{4,5,11,12}

$$ds^2 = -f dt^2 + \frac{m}{f} (dr^2 + r^2 d\theta^2) + \frac{m-n}{f} r^2 \sin^2 \theta \cos^2 \theta (\varepsilon_1 d\varphi_1 - \varepsilon_2 d\varphi_2)^2 + \frac{n}{f} r^2 \left[\sin^2 \theta \left(\varepsilon_1 d\varphi_1 - \frac{\omega}{r} dt \right)^2 + \cos^2 \theta \left(\varepsilon_2 d\varphi_2 - \frac{\omega}{r} dt \right)^2 \right], \quad (6)$$

where $\varepsilon_k = \pm 1$, $k = 1, 2$, denotes the sense of rotation in the k -th orthogonal plane of rotation.

The parametrization for the gauge potential, consistent with Eq. (6), is

$$A_\mu dx^\mu = a_0 dt + a_\varphi (\sin^2 \theta \varepsilon_1 d\varphi_1 + \cos^2 \theta \varepsilon_2 d\varphi_2). \quad (7)$$

All metric and gauge field functions depend on r only.

2.2. Boundary conditions

At infinity we impose on the metric the boundary conditions $f = m = n = 1$, $\omega = 0$, i.e., the solutions are asymptotically flat. For the gauge potential we choose a gauge, where $a_0 = a_\varphi = 0$.

The regular event horizon resides at a surface of constant radial coordinate, $r = r_H$ ^{3,4,5}, and is characterized by the condition $f(r_H) = 0$ ^{18,19,20,21,22,4,5}. Here the metric functions satisfy the boundary conditions $f = m = n = 0$, $\omega = r_H \Omega_H$, where Ω_H is (related to) the horizon angular velocity, defined in terms of the Killing vector

$$\chi = \xi + \Omega (\varepsilon_1 \eta_1 + \varepsilon_2 \eta_2), \quad (8)$$

which is null at the horizon. The gauge potential satisfies $\chi^\mu A_\mu|_{r=r_H} = \Phi_H$, $(da_\varphi/dr)_{r=r_H} = 0$, with constant horizon electrostatic potential Φ_H .

2.3. Global properties

Since the space-times we are considering are stationary, bi-axisymmetric, and asymptotically flat we may compute the mass M and the two angular momenta $J_{(k)}$ of the black holes by means of the Komar expressions associated with the respective Killing vector fields

$$M = \frac{-1}{16\pi G_5} \frac{3}{2} \int_{S_\infty^3} \alpha, \quad J_{(k)} = \frac{1}{16\pi G_5} \int_{S_\infty^3} \beta_{(k)}, \quad (9)$$

with $\alpha_{\mu\nu\rho} = \epsilon_{\mu\nu\rho\sigma\tau} \nabla^\sigma \xi^\tau$, $\beta_{(k)\mu\nu\rho} = \epsilon_{\mu\nu\rho\sigma\tau} \nabla^\sigma \eta_k^\tau$, and for equal-magnitude angular momenta $J_{(k)} = \varepsilon_k J$, $k = 1, 2$.

The electric charge Q associated with the Maxwell field can be defined by

$$Q = \frac{-1}{8\pi G_5} \int_{S_\infty^3} \tilde{F}, \quad (10)$$

with $\tilde{F}_{\mu\nu\rho} \equiv \epsilon_{\mu\nu\rho\sigma\tau} F^{\sigma\tau}$.

These global charges and the magnetic moment μ_{mag} , can be obtained from the asymptotic expansions of the metric and the gauge potential

$$f \rightarrow 1 - \frac{8G_5 M}{3\pi r^2}, \quad \omega \rightarrow \frac{4G_5 J}{\pi r^3}, \quad a_0 \rightarrow \frac{G_5 Q}{\pi r^2}, \quad a_\varphi \rightarrow -\frac{G_5 \mu_{\text{mag}}}{\pi r^2}. \quad (11)$$

The gyromagnetic ratio g is then defined via

$$g = 2 \frac{M \mu_{\text{mag}}}{Q J}. \quad (12)$$

2.4. Horizon properties

The expansion at the horizon shows, that the surface gravity κ

$$\kappa^2 = -\frac{1}{2} \lim_{r \rightarrow r_{\text{H}}} (\nabla_\mu \chi_\nu) (\nabla^\mu \chi^\nu) = \lim_{r \rightarrow r_{\text{H}}} \frac{f}{(r - r_{\text{H}}) \sqrt{m}} \quad (13)$$

is constant at the horizon, as required by the zeroth law of black hole mechanics, and that the electrostatic potential Φ_{H} is constant at the horizon as well. For equal-magnitude angular momenta, the area of the horizon A_{H} reduces to

$$A_{\text{H}} = 2\pi^2 r_{\text{H}}^3 \lim_{r \rightarrow r_{\text{H}}} \sqrt{\frac{m^2 n}{f^3}}. \quad (14)$$

To have a measure for the deformation of the horizon we consider the circumferences of the horizon, the polar circumference L_p , where φ_1 and φ_2 are kept constant, and the equatorial circumference, L_e , where $\theta = 0$ and φ_1 is kept constant (or equivalently $\theta = \pi/2$ and φ_2 is kept constant).

The horizon mass M_{H} and horizon angular momenta $J_{\text{H}(k)}$ are given by

$$M_{\text{H}} = \frac{-1}{16\pi G_D} \frac{3}{2} \int_{\mathcal{H}} \alpha, \quad J_{\text{H}(k)} = \frac{1}{16\pi G_D} \int_{\mathcal{H}} \beta_{(k)}, \quad (15)$$

where \mathcal{H} represents the surface of the horizon, and for equal-magnitude angular momenta $J_{\mathcal{H}(k)} = \varepsilon_k J_{\mathcal{H}}$, $k = 1, 2$. The mass M and angular momenta $J_{(k)}$ may thus be reexpressed in the form ^{6,10}

$$M = M_{\mathcal{H}} + M_{\Sigma} , \quad J_{(k)} = J_{\mathcal{H}(k)} + J_{\Sigma(k)} , \quad (16)$$

where $J_{\Sigma(k)}$ is a ‘bulk’ integral over the region of Σ outside the horizon, i.e., Σ is a space-like hypersurface with boundaries at spatial infinity and at the horizon.

These black holes satisfy the horizon mass formula

$$\frac{2}{3}M_{\mathcal{H}} = \frac{\kappa A_{\mathcal{H}}}{8\pi G_5} + 2\Omega J_{\mathcal{H}} , \quad (17)$$

and the Smarr formula ⁶

$$M = \frac{3}{2} \frac{\kappa A_{\mathcal{H}}}{8\pi G_5} + \frac{3}{2} 2\Omega J + \Phi_{\mathcal{H}} Q . \quad (18)$$

2.5. Scaling

The system of ODEs is invariant under the scaling transformation

$$r_{\mathcal{H}} \rightarrow \gamma r_{\mathcal{H}} , \quad \Omega \rightarrow \Omega/\gamma , \quad Q \rightarrow \gamma^2 Q , \quad a_{\varphi} \rightarrow \gamma a_{\varphi} , \quad (19)$$

with $\gamma > 0$ ^a. The solutions then have the scaling symmetry $\tilde{M} = \gamma^2 M$, $\tilde{J} = \gamma^3 J$, $\tilde{Q} = \gamma^2 Q$, $\tilde{r}_{\mathcal{H}} = \gamma r_{\mathcal{H}}$, $\tilde{\Omega} = \Omega/\gamma$, $\tilde{\kappa} = \kappa/\gamma$, etc.

We also note, that $\lambda \rightarrow -\lambda$ corresponds to $Q \rightarrow -Q$. Then, without loss of generality we will assume $\lambda \geq 0$ hereafter.

3. Numerical results

For the numerical calculations, we introduce the compactified radial variable $\bar{r} = 1 - r_{\mathcal{H}}/r$ ^{18,4}. We employ a collocation method for boundary-value ordinary differential equations, equipped with an adaptive mesh selection procedure ²³. Typical mesh sizes include $10^3 - 10^4$ points. The solutions have a relative accuracy of 10^{-10} . The set of numerical parameters to be fixed for a particular solution is $\{r_{\mathcal{H}}, \Omega, Q, \lambda\}$. By varying these parameters we generate families of EMCS black holes.

3.1. Domain of existence

Let us first consider the dependence of the domain of existence of EMCS black holes on the CS parameter λ . In Fig. 1 we exhibit the scaled angular momentum $|J|/M^{3/2}$ of extremal EMCS black holes versus the scaled charge Q/M for several values of λ : the pure EM case, $\lambda = 0$, the supergravity case, $\lambda = 1$, $\lambda = 1.5$, the second critical case, $\lambda = 2$, and $\lambda = 3$. For a given value of λ , black holes exist only in the regions bounded by the $J = 0$ -axis and by the respective solid curves, which are formed by extremal black holes.

^aNote, that for $D > 5$ the CS coupling constant is dimensionful and scales according to $\lambda \rightarrow \gamma^{n-2}\lambda$.

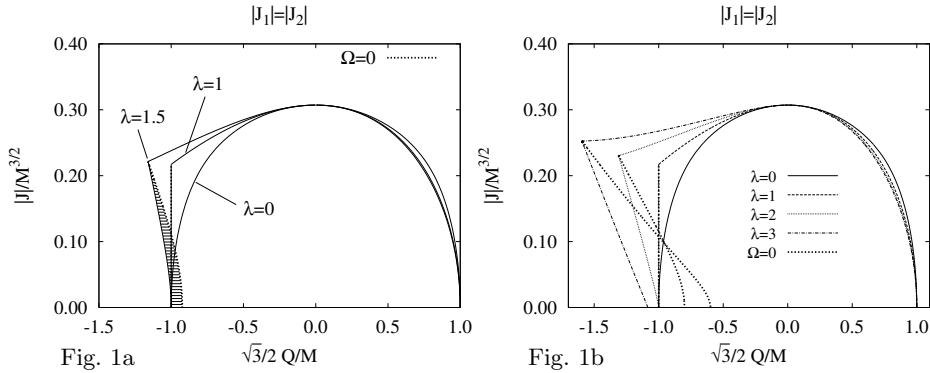


Fig. 1. Scaled angular momentum $J/M^{3/2}$ versus scaled charge Q/M for extremal EMCS black holes and $\Omega = 0$ solutions with CS coefficients $\lambda = 0, 1, 1.5, 2, 3$.

For fixed finite λ , there is an explicit asymmetry between solutions with positive and negative electric charge. The properties of EMCS black holes with positive Q are similar to those of EM black holes, whereas for EMCS black holes with negative Q surprising features are present.

As long as $\lambda < 1$ the boundary is smooth, but asymmetrical, unless λ vanishes. As λ approaches the supergravity value $\lambda = 1$, the boundary develops a kink, which turns into a singular point, when $\lambda = 1$. In the supergravity case the boundary then consists of two parts: a smooth curve and a straight vertical line, where both parts join at the singular point.

When $1 < \lambda \leq 2$, the static extremal black holes continue to reside at the lower left edge of the boundary of the domain of existence. But beyond the second critical value, $\lambda = 2$, they are located well within the domain of existence. (Recall that the static black holes are independent of λ .)

3.2. $\Omega = 0$ solutions

The staticity theorem of EM theory claims, that stationary non-rotating black holes (i.e., black holes with vanishing horizon angular velocity) are static²⁴. EMCS black holes, in contrast, may possess a static horizon, while their total angular momentum is non-vanishing^{8 b}.

Not present below $\lambda = 1$, these black holes arise in EMCS theory at the critical value λ_{SG} , where they constitute the left vertical boundary of the domain of existence. These $\lambda = 1$ solutions are very special, since they represent *supersymmetric* charged rotating black holes, where supersymmetry implies that the horizon must be non-rotating. Since $\Omega = 0$, these solutions possess no ergoregion.

^bBlack holes with static horizon and finite total angular momentum were first observed in Einstein-Maxwell-dilaton theory²⁵.

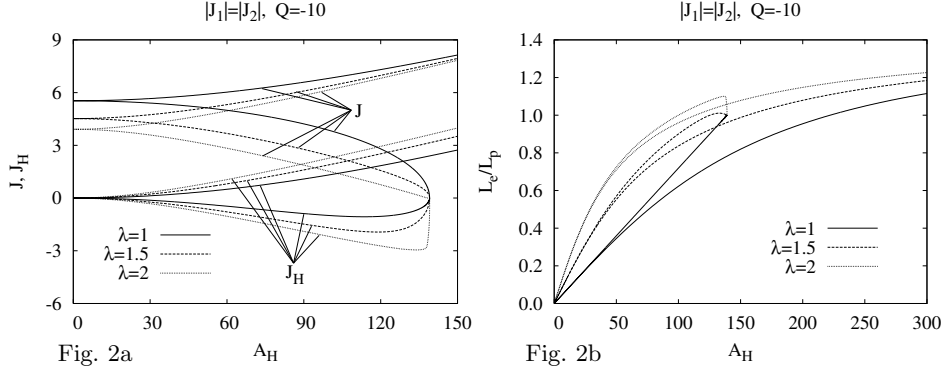


Fig. 2. Properties of (almost) extremal black holes ($\lambda = 1, 1.5, 2; Q = -10$). a) Total angular momentum J and horizon angular momentum J_H , b) deformation L_e/L_p , versus the area of the horizon A_H .

These supersymmetric black holes saturate the mass bound Eq. (4), and they satisfy the angular momentum bound Eq. (5). Thus while angular momentum is built up, the mass remains constant (for constant charge), in accordance with the first law, since $\kappa = \Omega = 0$.

As the total angular momentum is increased from its static limiting value $J = 0$, angular momentum is built up in the Maxwell field behind and outside the horizon, as seen in Fig. 2a, where the total angular momentum J and the horizon angular momentum J_H are exhibited. In particular, a negative fraction of the total angular momentum is stored in the Maxwell field behind the horizon⁶. Thus, while one expects frame dragging effects to cause the horizon to rotate, these effects are precisely counterbalanced by frame dragging effects, due to the negative contribution to the angular momentum by the fields behind the horizon, allowing these black holes to retain a static horizon¹⁰.

All these supersymmetric black holes possess a regular horizon, except for the limiting solution, saturating the bound Eq. (5). The area A_H of the horizon decreases as $|J|$ increases towards the bound Eq. (5), yielding a singular limiting solution with vanishing horizon area, $A_H = 0$. The effect of the rotation on the horizon is not to make it rotate, but to deform it from a round 3-sphere to a squashed 3-sphere as seen in Fig. 2b⁶.

Along the non-supersymmetric branch J and J_H have equal signs.

Below $\lambda = 1$ the only $\Omega = 0$ solutions are static black holes. At $\lambda = 1$, the supersymmetric black holes form a continuous set of non-static extremal $\Omega = 0$ solutions. As λ is increased beyond its supergravity value, the set of $\Omega = 0$ solutions becomes non-extremal, except for its extremal endpoint(s). The location of such sets of $\Omega = 0$ black holes within their respective domain of existence is indicated in Fig. 1 for several values of the CS coupling constant $\lambda > 1$.

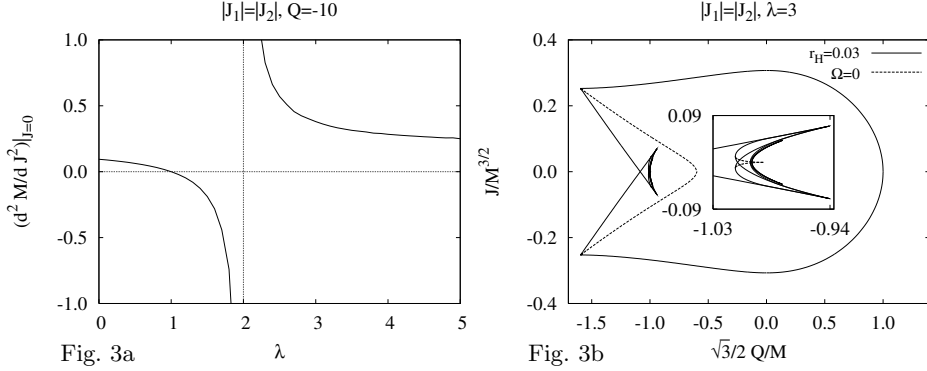


Fig. 3. a) Second-order derivative of the mass M with respect to the angular momentum J at $J = 0$ versus the CS coupling constant λ for extremal black holes ($Q = -10$). b) Scaled angular momentum $J/M^{3/2}$ versus scaled charge Q/M for (almost) extremal and $\Omega = 0$ solutions with CS coefficient $\lambda = 3$.

3.3. Instability

Extremal static EMCS black holes saturate the mass bound Eq. (4) for any value of λ . For stationary EMCS black holes demonstration of the bound Eq. (4) relied on the fact that $\lambda = 1$ ^{16,6}. While the mass bound Eq. (4) is respected by stationary black holes as long as $\lambda < 1$, it is violated, when $\lambda > 1$, as seen in Fig. 1.

As speculated before⁶, the mass can indeed decrease with increasing angular momentum for fixed $\lambda > 1$. Thus while an extremal static black hole with zero Hawking temperature and spherical symmetry cannot decrease its mass by Hawking radiation, it can however become unstable with respect to rotation, when $\lambda > 1$, with photons carrying away both energy and angular momentum to infinity. In terms of the first law as applied to $\lambda > 1$ extremal black holes ($\kappa = 0$) with fixed charge ($dQ = 0$), such an instability then requires, that the horizon is rotating in the opposite sense to the angular momentum, since $dM = \Omega_H \cdot dJ$ must be negative.

In Fig. 3a we demonstrate explicitly, that extremal static black holes can become unstable with respect to rotation, by exhibiting the deviation of the mass from the static value, computed via the second-order derivative of the mass with respect to the angular momentum at the extremal static solution. For $1 < \lambda < 2$ the mass is seen to decrease with increasing magnitude of the angular momentum for fixed electric charge, as attributed to the presence of counterrotating solutions, connected to the extremal static solution. Thus supersymmetry marks indeed the borderline between stability and instability.

3.4. Counterrotation

Responsible for the onset of instability, counterrotating black holes appear beyond the critical value $\lambda = 1$. For a given value of λ , the (main) set of rotating $\Omega = 0$ black holes (extending from a static solution to the corresponding extremal singular

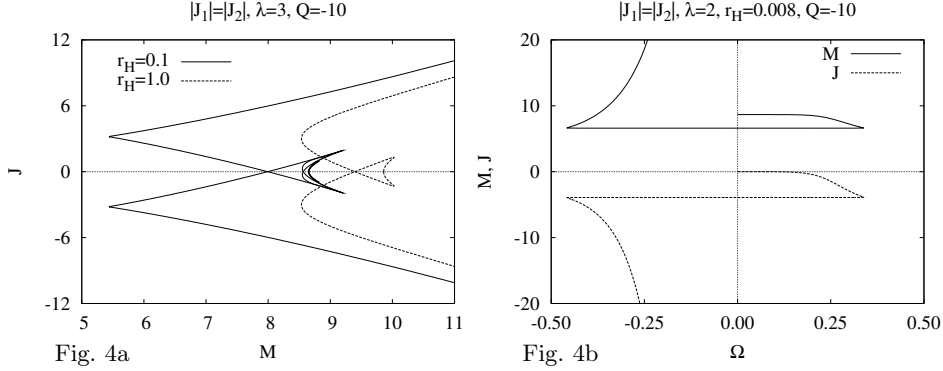


Fig. 4. a) Angular momentum J versus mass M for non-extremal black holes with horizon radii $r_H = 0.1$ and 1.0 ($\lambda = 3$; $Q = -10$). b) Angular momentum J and mass M versus horizon angular velocity Ω for almost extremal black holes ($\lambda = 2$, $r_H = 0.008$, $Q = -10$).

solution) then divides the domain of existence into two parts, as seen in Fig. 1. The right part contains ordinary black holes, where the horizon rotates in the same sense as the angular momentum, whereas the left part (the shaded region in Fig. 1a) contains black holes with unusual properties. When $1 < \lambda < 2$, all black holes in this region are counterrotating^c, i.e., their horizon rotates in the opposite sense to the angular momentum^{11,12}. When $\lambda \geq 2$ black holes with further intriguing features appear.

3.5. $J = 0$ black holes

As expected from the change in stability, another special case is reached, when $\lambda = 2$. Indeed, as λ reaches 2, another new phenomenon arises: a (continuous) set of rotating $J = 0$ solutions appears and persists as λ is increased beyond 2²⁷. The existence of these rotating $J = 0$ solutions relies on a special partition of the total angular momentum J , where the angular momentum within the horizon J_H is precisely equal and opposite to the angular momentum in the Maxwell field outside the horizon. In contrast, for $\lambda < 2$ only static $J = 0$ solutions exist. The presence of $J = 0$ solutions is seen in Figs. 3b and 4a for $\lambda = 3$.

Related to the $J = 0$ solutions, the domain of existence of EMCS black holes changes character, and extremal rotating $J = 0$ solutions replace extremal static solutions as the left edge of the boundary on the $J = 0$ axis, when $\lambda > 2$.

Thus beyond $\lambda = 2$ the set of extremal solutions not only forms the boundary of the domain of existence, but continues well within this domain, until the static extremal black hole is reached in a complicated pattern of bifurcating branches. Insight into this set is gained in Fig. 3b, where (almost) extremal solutions are

^cAlso counterrotating black holes were first observed in Einstein-Maxwell-dilaton theory²⁶.

exhibited for CS coefficient $\lambda = 3$, together with non-static $\Omega = 0$ solutions. Note, that all this new structure arises well within the counterrotating region, in the vicinity of the static extremal black holes.

With increasing λ an increasing number of such extremal rotating $J = 0$ black holes appears, and with them an increasing number of extremal $J \neq 0$ solutions with non-rotating horizon, each forming the end point of a whole set of (non-extremal) $\Omega = 0$, $J \neq 0$ black holes. Indeed, these sets of $\Omega = 0$ solutions always appear in pairs, connecting a static solution with an extremal solution, whose mass assumes an extremal value as well, in accordance with the first law.

The numerical data further indicate, that at the critical value $\lambda = 2$ a (continuous) set of extremal rotating $J = 0$ black holes with constant mass is present. This is illustrated in Fig. 4b. As the horizon angular velocity Ω increases, their mass M can remain constant, as long as $J = 0$, and the angular momentum is redistributed appropriately (as indicated by the steep rise of J_H in Fig. 2a). For these black holes, the deformation is oblate.

3.6. *Non-uniqueness*

Fig. 4a further reveals that beyond $\lambda = 2$ black holes are no longer uniquely characterized by their global charges. Thus the uniqueness conjecture does not hold for $D = 5$ EMCS stationary black holes with horizons of spherical topology, provided $\lambda > 2$ ^d. For $\lambda = 2$ even an infinite set of extremal black holes with the same global charges appears to exist, as numerical data indicate (see Fig. 4b).

3.7. *Four types of black holes*

To explore the properties of $\lambda > 2$ EMCS black holes further, let us now consider non-extremal black holes. We exhibit in Fig. 5 a set of solutions for $\lambda = 3$, possessing constant charge $Q = -10$ and constant (isotropic) horizon radius $r_H = 0.2$. Fig. 5a and 5b show the total angular momentum J and the horizon angular momentum J_H , respectively, as functions of the horizon angular velocity Ω , Fig. 5c and 5d show the corresponding masses M and M_H , and Fig. 5e and 5f the gyromagnetic ratio g and the deformation of the horizon as measured by the ratio of equatorial and polar circumferences L_e/L_p .

Fig. 5a exhibits the four types of rotating black holes, as classified by their total angular momentum J and horizon angular velocity Ω : Type I black holes correspond to the corotating regime, i.e., $\Omega J \geq 0$, and $\Omega = 0$ if and only if $J = 0$ (static). Type II black holes possess a static horizon ($\Omega = 0$), although their angular momentum does not vanish ($J \neq 0$). Type III black holes are characterized by counterrotation, i.e., the horizon angular velocity and the total angular momentum have opposite signs, $\Omega J < 0$. Type IV black holes, finally, possess a rotating horizon ($\Omega \neq 0$) but vanishing total angular momentum ($J = 0$).

^dThe previous counterexamples involved black rings ^{28,29,30,31,32}.

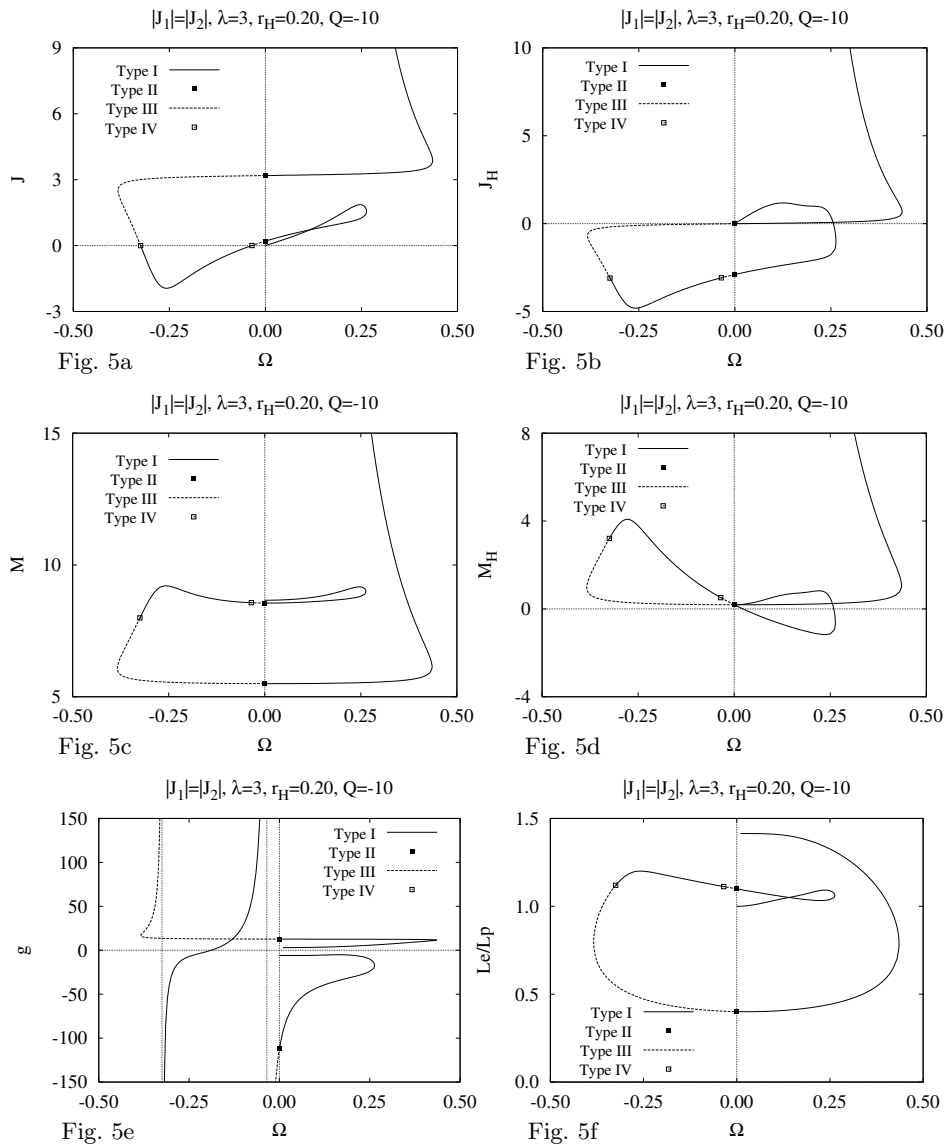


Fig. 5. Properties of non-extremal $\lambda = 3$ EMCS black holes with charge $Q = -10$ and horizon radius $r_H = 0.2$. a) Angular momentum J , b) horizon angular momentum J_H , c) mass M , d) horizon mass M_H , e) gyromagnetic ratio g , and f) ratio of horizon circumferences L_e/L_p versus horizon angular velocity Ω .

3.8. Negative horizon mass

As seen in Fig. 5b, the horizon angular momentum J_H of these black holes need not have the same sign as the total angular momentum J , and neither does the ‘bulk’ angular momentum J_Σ . As the horizon of the black hole is set into rotation,

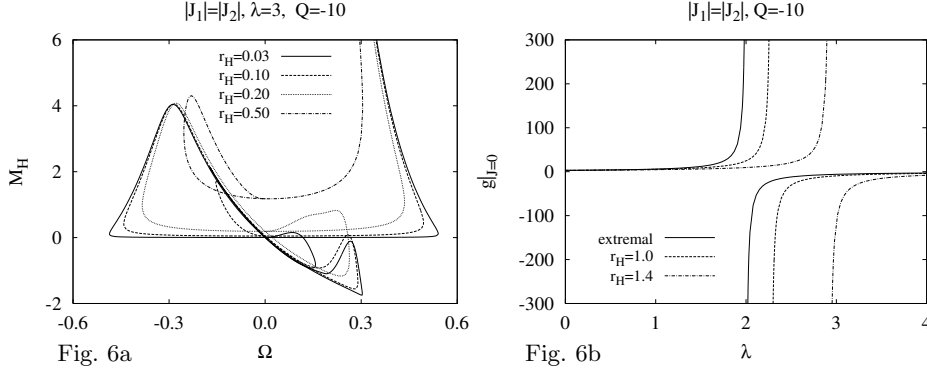


Fig. 6. a) Horizon mass M_H versus horizon angular velocity Ω for black holes with horizon radii $r_H = 0.03, 0.1, 0.2$ and 0.5 ($\lambda = 3; Q = -10$). b) Limiting value for $J \rightarrow 0$ of the gyromagnetic ratio g versus the CS coupling constant λ for black holes with $r_H = 0, 1, 1.4$ ($Q = -10$).

angular momentum is stored in the Maxwell field both behind and outside the horizon, yielding a rich variety of configurations. Starting from the static solution, a corotating branch evolves, along which J_H and J_Σ have opposite signs. After the first bifurcation Ω moves back towards zero and so does J , but both J_H and J_Σ remain finite, retaining part of their built up angular momentum and thus their memory of the path, like in a hysteresis. This is important, since when moving Ω continuously back to and beyond zero, the total angular momentum follows and changes sign as well. The horizon angular momentum, however, retains its sign. Thus the product ΩJ_H turns negative and remains negative up to the next bifurcation and still further, until Ω reaches again zero.

The presence of $\Omega J_H < 0$ solutions explains the occurrence of black holes with negative horizon mass, $M_H < 0$, which are exhibited in Fig. 5d. The correlation between $\Omega J_H < 0$ and $M_H < 0$ black holes is evident here. In fact, the sets of $\Omega J_H < 0$ and $M_H < 0$ black holes almost coincide, when κA_H is small, as seen from the horizon mass formula Eq. (17). The angular momentum stored in the Maxwell field behind the horizon is thus responsible for the negative horizon mass of the black holes. The total mass is always positive, however, as seen in Fig. 5c.

For larger values of r_H the set of negative horizon mass black holes decreases, while it increases for smaller values of r_H , as seen in Fig. 6a. In fact, as r_H decreases, more branches of solutions appear in the vicinity of the static solution, giving rise to more branches of negative horizon mass black holes.

3.9. Gyromagnetic ratio

Another interesting feature of these charged rotating EMCS black holes is their gyromagnetic ratio g , exhibited in Fig. 5e. When $\lambda > 2$, the gyromagnetic ratio is unbounded, reaching any real value including zero. The main consequence of this is that, contrary to pure EM theory, a vanishing total angular momentum does not

readily imply a vanishing magnetic moment and viceversa.

The gyromagnetic ratio is thus another indicator of the particularity of $\lambda = 2$, as also seen in Fig. 6b.

4. Conclusions

Stationary black holes of EM theory in 4 dimensions now appear to be very special, since their familiar properties are not shared in general by black holes in higher dimensions or by black holes in the presence of more or different fields.

4.1. $D = 5$ EMCS black holes

Charged rotating black holes of EMCS theory in five dimensions, which are asymptotically flat with a regular horizon of spherical topology, can exhibit remarkable features. Classifying the EMCS black holes by their total angular momentum J and horizon angular velocity Ω , four types of black holes arise: I. corotating black holes, i.e., $\Omega J \geq 0$, for all values of λ , II. black holes with static horizon and non-vanishing total angular momentum, i.e., $\Omega = 0$, $J \neq 0$, for $\lambda \geq 1$, III. counterrotating black holes, where the horizon angular velocity and the total angular momentum have opposite signs, i.e., $\Omega J < 0$, for $\lambda > 1$, and IV. black holes with rotating horizon and vanishing total angular momentum, i.e., $\Omega \neq 0$, $J = 0$, for $\lambda \geq 2$.

As the horizon of static EMCS black holes is set into rotation, angular momentum is stored in the Maxwell field both behind and outside the horizon. Following paths through configuration space, the horizon angular momentum J_H and the ‘bulk’ angular momentum J_Σ can retain part of the angular momentum built up in the Maxwell field, even when the horizon angular velocity vanishes again. Thus they retain the memory of the path, like a hysteresis. Consequently, solutions with $\Omega J_H < 0$ appear, which possess a negative horizon mass $M_H < 0$, as long as κA_H is sufficiently small. Thus the angular momentum stored in the Maxwell field behind the horizon is responsible for the negative horizon mass of these black holes. Their total mass is positive, however ^e.

Moreover, these EMCS black holes are no longer uniquely characterized by their global charges, i.e., the uniqueness conjecture does not hold in general for stationary black holes with horizons of spherical topology; and their gyromagnetic ratio may take any real value, including zero.

4.2. $D = 4$ EMD black holes

A number of features of $D = 5$ EMCS black holes appear also for $D = 4$ EMD black holes, with dilaton coupling constant γ , when both electric (Q) and magnetic (P) charge are present ²⁶. In EMD theory the Kaluza-Klein value $\gamma = \sqrt{3}$ represents

^eThe occurrence of a negative horizon mass has been also reported recently in the context of $4D$ black holes surrounded by perfect fluid rings ³³.

the (first) critical value. For $\gamma < \sqrt{3}$ only corotating black holes exist. For $\gamma = \sqrt{3}$ stationary black holes with non-rotating horizon appear and form the vertical part of the boundary ²⁵. Their angular momentum is bounded by $|J| \leq |PQ|$ (analogous to Eq. (5)). For $\gamma > \sqrt{3}$ corotating and counterrotating black holes exist ²⁶. Thus in EMD theory the Kaluza-Klein value $\gamma = \sqrt{3}$ marks the change from stability to instability. Stationary $\Omega = 0$ black holes and counterrotating black holes also exhibit squashed horizons ²⁶.

Whether also $J = 0, \Omega \neq 0$ solutions are present, whether uniqueness is violated, or whether negative horizon mass black holes are present remains to be investigated.

4.3. $D > 5$ EMCS black holes

All these intriguing new types of stationary $5D$ EMCS black holes occur also for EMCS black holes in higher odd dimensions ¹². But since the CS coefficient then becomes dimensionful, it changes under scaling transformations Eq. (19), unless $\lambda = 0$. Thus any feature present for a certain non-vanishing value of λ will be present for any other non-vanishing value (although for the correspondingly scaled value of the charge). For that reason, the critical behaviour of the solutions cannot be classified by λ alone, but only by a scale invariant ratio involving λ ¹².

Interestingly, in $D = 9$, a further type of black holes appears: V. non-static $\Omega = J = 0$ black holes, possessing a finite magnetic moment ¹². Clearly, further surprises may be waiting in higher dimensions.

Acknowledgments

FNL gratefully acknowledges Ministerio de Educación y Ciencia for support under grant EX2005-0078.

References

1. S. Dimopoulos, and G. Landsberg, Phys. Rev. Lett. **87** (2001) 161602.
2. S. B. Giddings, and S. Thomas, Phys. Rev. **D65** (2002) 056010.
3. R. C. Myers, and M. J. Perry, Ann. Phys. (N.Y.) **172** (1986) 304.
4. J. Kunz, F. Navarro-Lérida, and A. K. Petersen, Phys. Lett. **B614** (2005) 104.
5. J. Kunz, F. Navarro-Lérida, and J. Viebahn, Phys. Lett. **B 639** (2006) 362.
6. J. P. Gauntlett, R. C. Myers, and P. K. Townsend, Class. Quantum Grav. **16** (1999) 1.
7. J. C. Breckenridge, D. A. Lowe, R. C. Myers, A. W. Peet, A. Strominger, and C. Vafa, Phys. Lett. **B381** (1996) 423.
8. J. C. Breckenridge, R. C. Myers, A. W. Peet, and C. Vafa, Phys. Lett. **B391** (1997) 93.
9. C. A. R. Herdeiro, Nucl. Phys. **B582** (2000) 363.
10. P. K. Townsend, Annales Henri Poincare **4** (2003) 183.
11. J. Kunz, and F. Navarro-Lérida, Phys. Rev. Lett. **96** (2006) 081101.
12. J. Kunz, and F. Navarro-Lérida, Negative horizon mass for rotating black holes, hep-th/0610036.

13. M. Cvetič, H. Lü, and C. N. Pope, Phys. Lett. **B598** (2004) 273.
14. M. Cvetič, H. Lü, and C. N. Pope, Phys. Rev. **D70** (2004) 081502.
15. Z.-W. Chong, M. Cvetič, H. Lü, and C. N. Pope, Phys. Rev. Lett. **95** (2005) 161301.
16. G.W. Gibbons, D. Kastor, L.A.J. London, P.K. Townsend, and J. Traschen, Nucl. Phys. **B416** (1994) 850.
17. A. N. Aliev, and V. P. Frolov, Phys. Rev. **D69** (2004) 084022.
18. B. Kleihaus, and J. Kunz, Phys. Rev. Lett. **86** (2001) 3704.
19. B. Kleihaus, J. Kunz, and F. Navarro-Lérida, Phys. Rev. **D66** (2002) 104001.
20. B. Kleihaus, J. Kunz, and F. Navarro-Lérida, Phys. Rev. Lett. **90** (2003) 171101.
21. B. Kleihaus, J. Kunz, and F. Navarro-Lérida, Phys. Rev. **D69** (2004) 064028.
22. B. Kleihaus, J. Kunz, and F. Navarro-Lérida, Phys. Lett. **B599** (2004) 294.
23. U. Ascher, J. Christiansen, and R. D. Russell, Mathematics of Computation 33 (1979) 659; ACM Transactions 7 (1981) 209.
24. R. M. Wald, College Park 1993, Directions in general relativity **1** 358.
25. D. Rasheed, Nucl. Phys. **B454** (1995) 379;
26. B. Kleihaus, J. Kunz, and F. Navarro-Lérida, Phys. Rev. **D69** (2004) 081501.
27. O. Brodbeck, M. Heusler, N. Straumann, and M. S. Volkov, Phys. Rev. Lett. **79** (1997) 4310.
28. R. Emparan, and H. S. Reall, Phys. Rev. Lett. **88** (2002) 101101.
29. H. Elvang, Phys. Rev. **D68** (2003) 124016.
30. H. Elvang, and R. Emparan, J. High Energy Phys. **0311** (2003) 035.
31. R. Emparan, J. High Energy Phys. **0403** (2004) 064.
32. S. S. Yazadjiev, Phys. Rev. **D73** (2006) 104007.
33. M. Ansorg, and D. Petroff, Negative Komar mass, gr-qc/0607091.